BMC Oral Health

RESEARCH

Open Access

Automatic maxillary sinus segmentation and age estimation model for the northwestern Chinese Han population

Yu-Xin Guo[1†], Jun-Long Lan[1†], Wen-Qing Bu[1,2], Yu Tang[1,2], Di Wu[1,2], Hui Yang[1,2], Jia-Chen Ren[1,2], Yu-Xuan Song[3], Hong-Ying Yue[1], Yu-Cheng Guo[1,2*] and Hao-Tian Meng[1,2*]

Abstract

Background Age estimation is vital in forensic science, with maxillary sinus development serving as a reliable indicator. This study developed an automatic segmentation model for maxillary sinus identification and parameter measurement, combined with regression and machine learning models for age estimation.

Methods Cone Beam Computed Tomography (CBCT) images from 292 Han individuals (ranging from 5 to 53 years) were used to train and validate the segmentation model. Measurements included sinus dimensions (length, width, height), inter-sinus distance, and volume. Age estimation models using multiple linear regression and random forest algorithms were built based on these variables.

Results The automatic segmentation model achieved high accuracy, which yielded a Dice similarity coefficient (DSC) of 0.873, an Intersection over Union (IoU) of 0.7753, a Hausdorff Distance 95% (HD95) of 9.8337, and an Average Surface Distance (ASD) of 2.4507. The regression model performed best, with mean absolute errors (MAE) of 1.45 years (under 18) and 3.51 years (aged 18 and above), providing relatively precise age predictions.

Conclusion The maxillary sinus-based model is a promising tool for age estimation, particularly in adults, and could be enhanced by incorporating additional variables like dental dimensions.

Keywords Age estimation, Forensic anthropology, Maxillary sinus, Automatic segmentation, Machine learning

Background

Age estimation is a crucial aspect in forensic science, essential for individual identification, and it also bears legal implications for individuals without identification documents in certain countries, such as Germany [1, 2]. Researchers have attempted to estimate age using various methods for a long time [2–7], with approaches based on the developmental stage of joints and bones, like the epiphyseal growth plate, proving to be accurate for juveniles but less reliable for adults [4, 8]. As a complementary approach, DNA methylation offers the potential to enhance the accuracy of age estimation in adults [7]. However, the DNA methylation testing process is

†Yu-Xin Guo and Jun-Long Lan contributed equally to this work.

*Correspondence:
Hao-Tian Meng
menghaotian0803@126.com
[1]Key Laboratory of Shaanxi Province for Craniofacial Precision Medicine Research, College of Stomatology, Xi'an Jiaotong University, 98 XiWu Road, Xi'an 710004, Shaanxi, People's Republic of China
[2]Department of Orthodontics, College of Stomatology, Xi'an Jiaotong University, 98 XiWu Road, Xi'an 710004, Shaanxi, People's Republic of China
[3]College of Forensic Science, Xi'an Jiaotong University, Xi'an 710061, Shaanxi, People's Republic of China

complex and requires significant time and costly equipment, presenting challenges for both laboratory facilities and personnel [13]. This restricts the widespread use of the technology. Additionally, DNA methylation is limited in its applicability to old or highly degraded samples, where extracting high-quality DNA is difficult [14]. Consequently, there is an urgent need to develop more convenient and cost-effective methods for age estimation, especially for adults.

Some studies indicated that the maxillary sinus often remains intact when other skeletal structures have sustained extensive damage, possessing great potential in forensic identification [15, 16]. Research leveraging the maxillary sinus across different parameters has been conducted, such as investigations that utilized the sexual dimorphism of maxillary sinus to predict the sex of human remains [17–19]. Moreover, the architecture of the maxillary sinus is intimately associated with age. Throughout the ontogenetic trajectory of Homo sapiens, the maxillary sinus undergoes progressive enlargement during minority. Subsequent to the attainment of adulthood, however, it experiences a gradual regression in size [20, 21]. This phenomenon suggests that the maxillary sinus is subject to morphological transformation with advancing age, hence facilitating the potential employment of its mensurative data for the estimation of chronological age. The preponderance of current research was confined to the examination of the interrelationship between age and the dimensions of the maxillary sinus, with a paucity of studies attempting to utilize such data for the purposes of age estimation [22].

A lot of studies of individual identification in forensic medicine can hard put into service widely because of some reasons like high costs and professional requirements. Therefore, one technology couldn't achieve widespread application if it doesn't achieve low cost and standardization of data measurement. As mentioned above, the high cost and sample quality requirement of DNA methylation testing technology make it just suitable for some special cases. With the innovation of Computed Tomography (CT), micro-Computed Tomography (micro-CT) and Cone Beam CT (CBCT), the lower cost of imaging testing made it more and more popular with studies of forensic medicine [5, 8, 18, 19, 22]. Then the only difficulty which hinders its wide application is how to achieve the standard measurement of data. For grassroots judicial staff, it is too difficult to achieve standard measurement or staging for special tissues. On the other hand, even professionals couldn't ensure that the measurements are exactly same in some cases. However, if this task is entrusted to machine learning, the outcome is likely to be more favorable. The application of machine learning in the medical field is already widespread, encompassing areas such as drug development and image analysis [23, 24]. This study leveraged the advantages of machine learning to apply it in the identification and segmentation of the maxillary sinus, as well as in the construction of age estimation models.

With the advancement of deep learning, it has become feasible to perform three-dimensional medical image segmentation using semi-supervised learning (SSL) [25–28]. The journey began with the deployment of UNet, a pioneering deep learning model for image segmentation, in medical image applications [29]. Following this, UA-MT integrated SSL into the segmentation process [30]. Building on these foundations, contemporary methodologies such as MCF and BCP have further validated the potential of SSL approaches for precise medical image segmentation [31, 32]. Progressive Mean Teacher (PMT), a cutting-edge research development in this field, introduces a progressive design that fosters stable model diversity through temporal differences, achieving the state-of-the-art results [33]. Owing to the user-friendly deployment of the PMT code, it was selected as the medical image segmentation model for this study. According to the results presented in this research, an ample yet not excessive quantity of supervised data significantly enhanced the model's training regimen. Nonetheless, PMT is capable of delivering commendable performance even when the proportion of available supervised data is reduced.

Consequently, the objective of the present study was to develop an image segmentation model that can automatically measure the maxillary sinus data from CBCT images. These measurements will then be harnessed to create an age estimation model, which aimed to accurately predict the ages of individuals. This model was designed to be accessible to basic level judicial officials, enabling them to perform age estimation without the need for specialized knowledge of human anatomy.

Methods

Samples selection and ethical declaration

In this study, samples were selected from the Department of Oral Radiology, Stomatology Hospital of Xi'an Jiaotong University, and their whole CBCT images were further collected after the acquisition of written informed consents and demographic information. All CBCT scans were taken by the Cone-beam X-ray Computed Tomography System (KaVO 3D eXam I, Germany), and exported into DICOM format (Digital Imaging and Communications in Medicine, an international standard for medical images and related information). The current research was conducted after the approval of the Biomedical Ethics Committee of Xi'an Jiaotong University Health Science Center, China (No: [2021] 1473). The inclusion criteria were as follows:

(1) Living in the northwest region of China, without trauma, surgery, deformities, systemic diseases, or malnutrition.
(2) The left and right maxillary sinuses were both scanned intact.
(3) The patient's complete personal information must be acquired.
(4) The boundary between the maxillary sinus and surrounding tissues must be clear.
(5) There is no severe inflammation in the maxillary sinus.
(6) There are no broken teeth in the maxillary sinus.

Data measurement

Training of automatic segmentation model for maxillary sinus

In alignment with the guidelines for the application of artificial intelligence in dentistry as proposed by Schwendicke, this study adhered to the established protocols [34]. And the model training methods referred to Zhou et al. study [33]. All CBCT images of the maxillary sinus were processed using ITK-SNAP 4.0.2 (Penn Image Computing and Science Laboratory, USA). A selection of 40 CBCT images were chosen for manual labeling of the maxillary sinus, as depicted in Fig. 1. The remaining images were archived in "nii.gz" format for subsequent utilization.

To facilitate normalization, the pixel grayscale values of the images, which originally ranged from − 1000 to 2000 were transformed into the "0-255" scale. Post-normalization the image format was converted to "int 8" to enhance the efficiency of model data processing. These processed images were then stored alongside the manually labeled counterparts in "h5" file documents. Additionally, to focus on the relevant areas, the images were cropped, as illustrated in Fig. 2 (a: original image; b: cropped image).

Regarding the training specifics, PMT was used to train on the entire dataset, which comprised 76 samples, with 24 of them being supervised. To validate the model's successful training and its potential for deployment on a broader dataset, an additional 4 samples were chosen for testing. The model underwent a total of 6000 training iterations, with the learning rate to 0.1 of its original value every 2500 iterations. The two student models within the PMT framework were utilized, with their inference results combined to produce the final model inference output.

Following the acquisition of the model's inference results, the output labels were meticulously analyzed. By examining the connected regions within the segmentation and calculating the voxel volume, the two most prominent segments were identified as the model's final segmentation outcomes, effectively mitigating the impact of noise in the output.

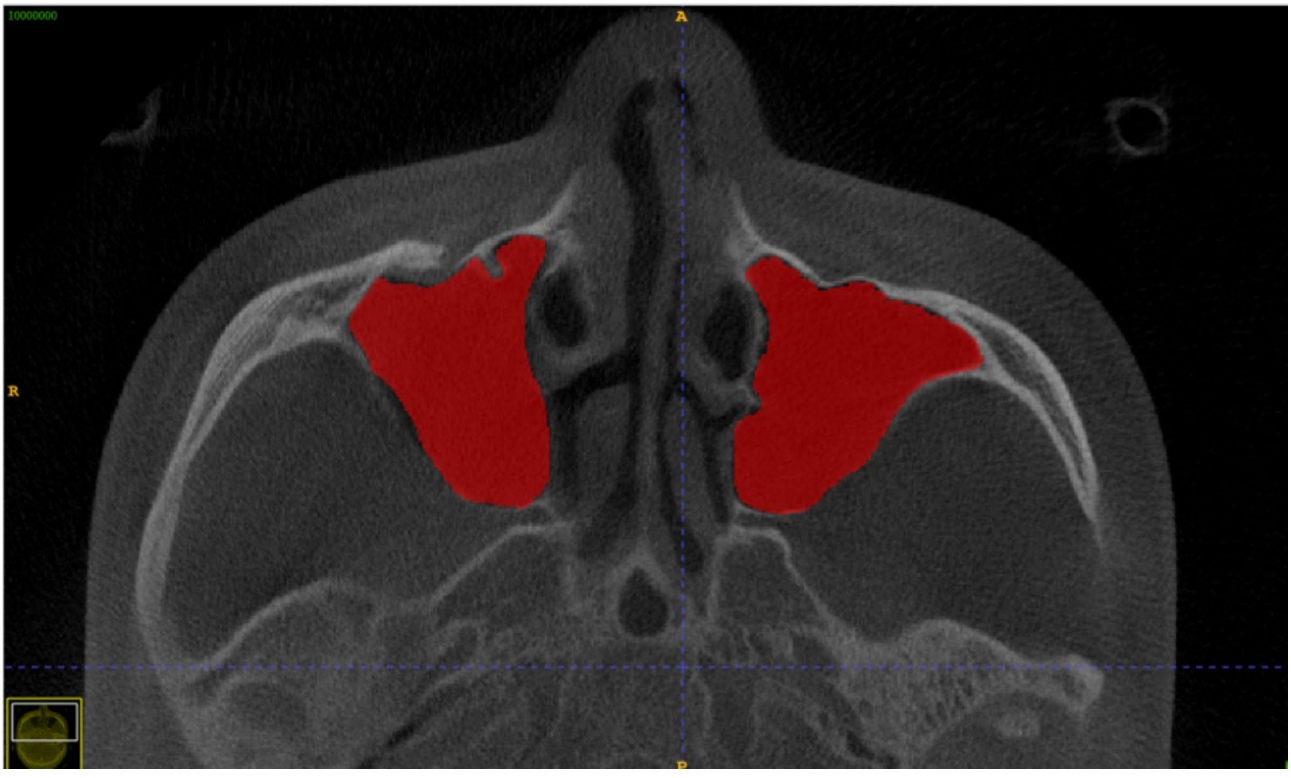

Fig. 1 The maxillary sinus labeled in CBCT manually

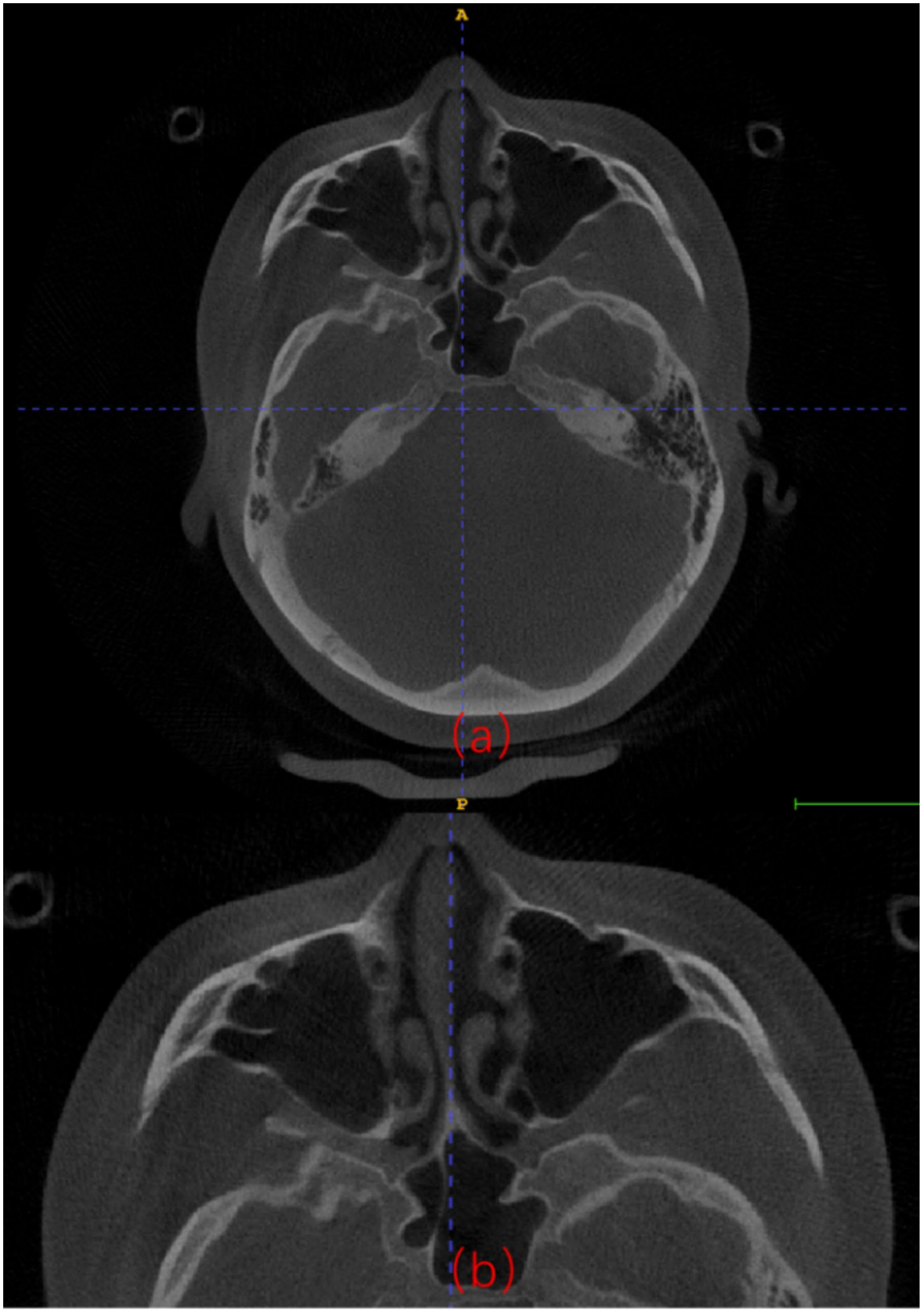

Fig. 2 The cropped CBCT images

To assess segmentation performance, traditional evaluation metrics were employed, including the Dice similarity coefficient (DSC), Intersection over Union (IoU), 95% Hausdorff Distance (95HD), and Average Surface Distance (ASD). The DSC quantifies the quality of the segmentation results by determining the ratio of intersection to the union of the predicted and actual values, with a score ranging from 0 to 1. A higher DSC denotes superior segmentation performance. IoU measures the similarity between two sets by calculating the ratio of their intersection to their union, with values ranging from 0 (no intersection) to 1 (completely identical). 95HD is utilized to gauge the accuracy of segmentation boundaries, with a smaller value indicating higher accuracy. ASD refers to the average distance of all points in an image, and a smaller ASD value reflects excellent segmentation precision. The efficiency of maxillary sinus segmentation was evaluated based on the average outcomes from the four test samples, providing a robust indicator of the model's performance.

Measurement of maxillary sinus

Linear measurements were conducted in accordance with Otsuki's standards [22], including the following parameters: the maximum linear length of the maxillary sinus (MSL, as seen in Fig. 3a), representing the distance between the anterior and posterior points of the inner wall of the maxillary sinus; the maximum linear width of the maxillary sinus (MSW, illustrated in Fig. 3b), which is the distance from the lateral outermost point to the innermost point of a single maxillary sinus; the inter-lateral distance of the maxillary sinus (refer to as "distance", depicted in Fig. 3d), signifying the separation between the lateral outermost points of two maxillary sinuses across consecutive cross-section images; and the maximum linear height of the maxillary sinus in sequential coronal plane images (MSH, shown in Fig. 3c), which is the vertical distance from the apex to the base of the maxillary sinus inner wall; finally, the volume of the maxillary sinus is determined by segmenting the maxillary sinus images at each slice and summing these slices to obtain the total volume (refer to as "volume").

Statistical analysis and age estimation model construction

In this research, all data analysis were conducted using R v.4.3.1 and all the samples were divided into two age-based groups: those aged 18 and above (comprising 82 males and 78 females) and those under 18 years old (consisting of 58 males and 74 females). The normality of the data was assessed using the Shapiro-Wilk test, followed by the computation of descriptive statistics. Scatterplot of each variable was generated to observe their correlation with age intuitively. The Pearson correlation test was then employed to examine the linear relationship between

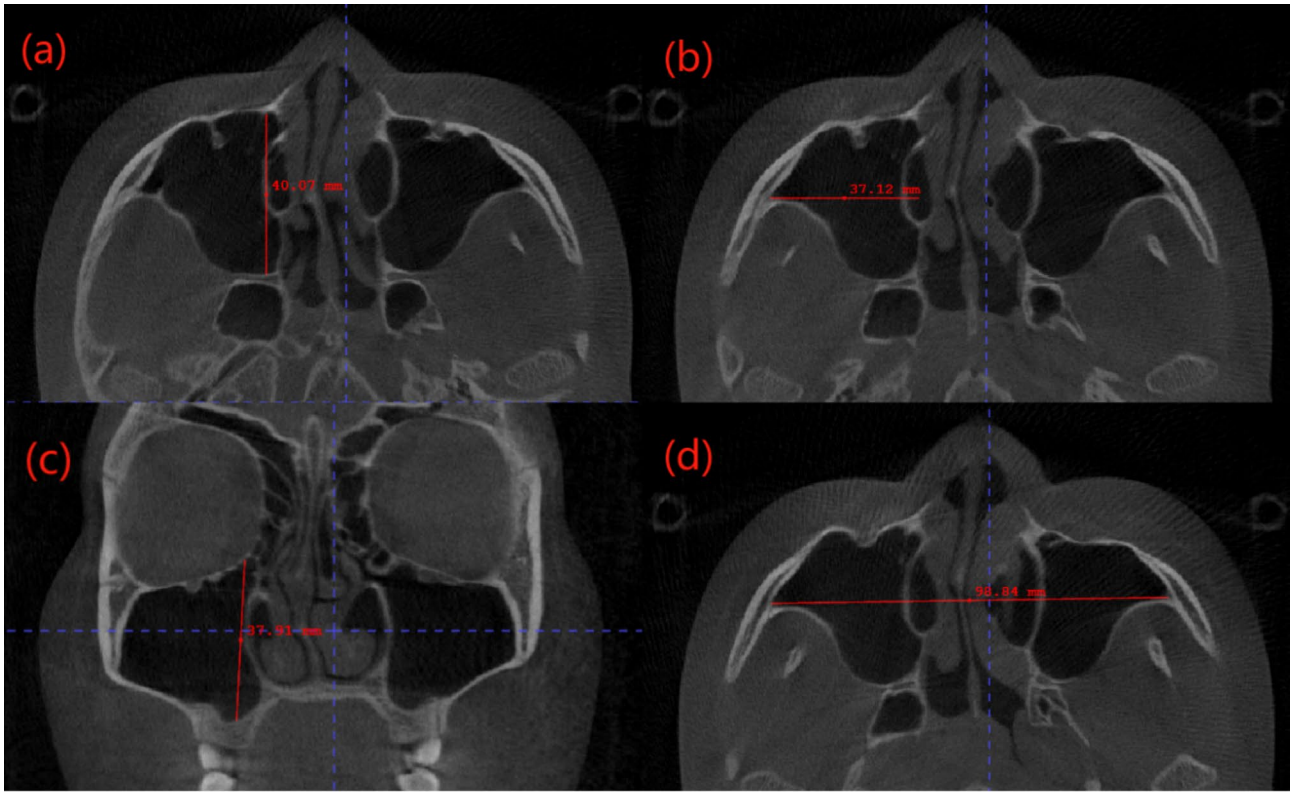

Fig. 3 Linear variables of maxillary sinus

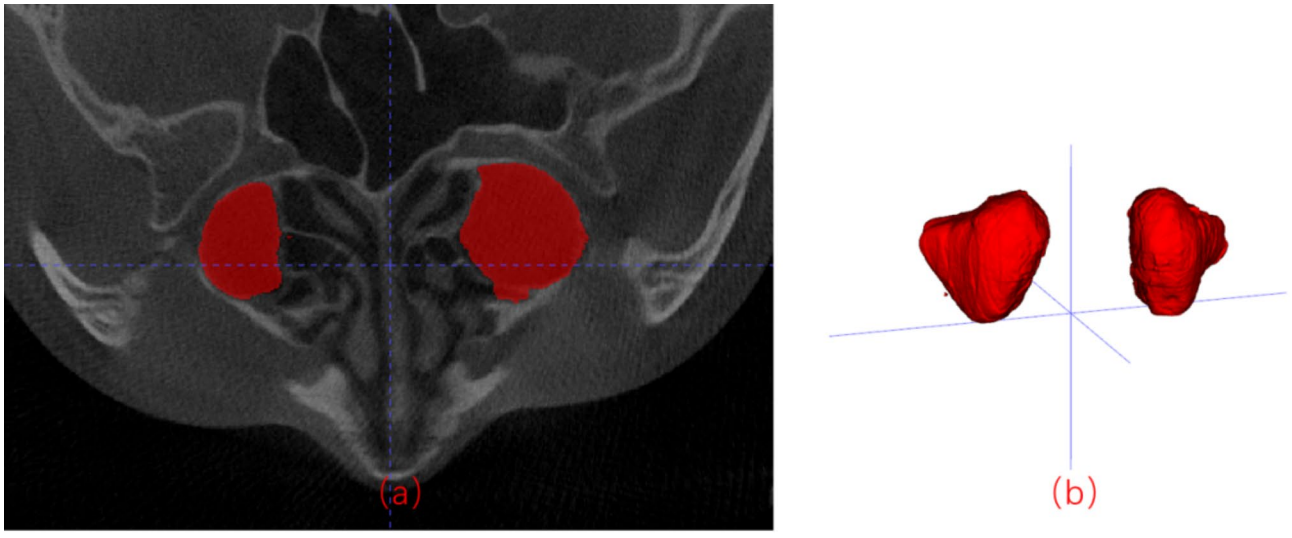

Fig. 4 Maxillary sinus cropped by automatic segmentation model

Table 1 Evaluating indicators of automatic segmentation model

index	DSC	IoU	95HD	ASD
Segmentation model	0.873	0.7753	9.8337	2.4507

each variable and age. Independent sample t-tests were carried out to determine the differences in each variable between males and females. Variables that were found to be statistically significant were subsequently integrated as predictive factors into the age estimation model. For this purpose, both the random forest algorithm and multiple linear regression were utilized to construct predictive models. Through parameters optimization, the models with the highest predictive accuracy were selected. To evaluate the accuracy of the age estimation, mean absolute error (MAE) was adopted as the metric of choice.

Results

Demographic data

In this research, a cohort of 292 individuals of Han ethnicity was assembled from the Department of Oral Radiology, Stomatology Hospital of Xi'an Jiaotong University, including 58 males and 74 females ranging in age from 4 to 17 years, as well as 82 males and 78 females aged between 18 and 53 years. Their CBCT images were meticulously collected for analysis.

Efficiency of Automatic Segmentation Model for Maxillary Sinus.

The automatic segmentation model has successfully delineated the maxillary sinus from CBCT images, as shown in Fig. 4. Four relevant indicators were utilized to evaluate its segmentation efficiency, of which DSC = 0.873, IoU = 0.7753, 95HD = 9.8337 and ASD = 2.4507, which collectively reflected a commendable level of segmentation performance (refer to Table 1). Utilizing automatic segmentation model, the linear dimensions and volume of the maxillary sinus could be measured swiftly and accurately.

Sex differences

All variables conformed to a normal distribution, as indicated by the Shapiro-Wilk test results ($p > 0.05$), as shown in Table 2. Descriptive statistics analysis revealed that, within the 18 and above age group, males exhibited higher mean values for each variable compared to females. In contrast, no discernible differences were observed between males and females in the under 18 age group (refer to Table 3). This pattern was further supported by the independent samples t-test, which yielded similar conclusions. Specifically, for the 18 and above age group, there were significant differences between males and females across all variables ($p < 0.05$), as shown in Table 2. However, in the under 18 age group, all variables showed no significant differences between males and females, as evidenced by p-values exceeding 0.05 (Table 2).

Regression fitting

By observing scatterplot of each variable in Fig. 5, it was evident that a distinct linear relationship existed between age and each variable within the under 18 age group. However, such a relationship was less apparent in the 18 and above age group. The Pearson correlation test proved these observations, demonstrating that every variable was significantly correlated with age in the under 18 group, whereas only "L_MSL, R_MSL, R_MSW, R_MSH" exhibited significant correlation in the 18 and above group (Table 2). Then variables correlated significantly with age were utilized to fit age estimation models in each group. In the under 18 age group, all variables served as influential factors in the models, with

Table 2 Shapiro-Wilk test, independent samples t-test, Pearson correlation test results

Index		S-W test		Independent t-test with sex		Pearson correlation test with age	
		w	*p*-value	t	*p*-value	t	*p*-value
Under 18 years old	L_MSL	0.9872	0.2594	-0.7667	0.4446	5.1344	<0.0001
	L_MSW	0.9877	0.2877	-0.1023	0.9187	3.8786	0.0002
	L_MSH	0.9855	0.1754	-0.2992	0.7652	7.6928	<0.0001
	R_MSL	0.9909	0.5461	-0.9866	0.3257	4.9953	<0.0001
	R_MSW	0.9850	0.1571	-1.3060	0.1939	4.1490	<0.0001
	R_MSH	0.9943	0.8792	0.3661	0.7149	7.0924	<0.0001
	L_volume	0.9947	0.9078	1.7985	0.0744	5.8481	<0.0001
	R_volume	0.9930	0.7636	0.3859	0.7002	8.6591	<0.0001
	distance	0.9872	0.2575	-1.4279	0.1557	6.8206	<0.0001
Aged 18 and above	L_MSL	0.9915	0.4745	-5.9307	<0.0001	-2.0576	0.0414
	L_MSW	0.9902	0.3571	-3.8918	0.0001	-0.4964	0.6204
	L_MSH	0.9899	0.3250	-4.1075	<0.0001	-1.9707	0.0506
	R_MSL	0.9851	0.0923	-4.7916	<0.0001	-3.2428	0.0015
	R_MSW	0.9938	0.7463	-4.2086	<0.0001	-2.7848	0.0060
	R_MSH	0.9846	0.0810	-5.3320	<0.0001	-2.3138	0.0220
	L_volume	0.9879	0.1941	-3.3623	0.0010	-1.5839	0.1153
	R_volume	0.9898	0.3198	-4.3848	<0.0001	-1.5323	0.1276
	distance	0.9925	0.5966	-5.5857	<0.0001	-1.2518	0.2126

both multiple linear regression and random forest algorithms been employed for model fitting. The multiple linear regression model exhibited strong performance, with a MAE of 1.45 years between predicted and actual age of the test group, while that of random forest model was 1.62 years (listed in Table 4). In the 18 and above age group, only four indexes were utilized for model fitting. The testing result mirrored the performance of the under 18 age group, with the multiple linear regression model yielding an MAE of just 3.51 years, while the random forest model's MAE was 3.84 years (Table 4).

Discussion

Age estimation in forensic science remains a challenge, particular for adults. Current methods based on bone growth [6, 8] and DNA methylation [13, 14] have limitations. This study proposes a novel method for age estimation using the maxillary sinus, which maintains integrity even after damage [15, 16]. The parameters of maxillary sinus had been shown to correlate with age in this research, and with advancements in imaging technology, its measurement has become more accessible.

In this research, an automatic segmentation model was constructed for maxillary sinus in order to collect linear data and volume of maxillary sinus rapidly and properly. Our preliminary research indicated that the PMT surpassed various leading segmentation techniques, including VNet, UA-MT, SASSNet, DTC, BCP, and MCF. VNet served as the benchmark for comparison [31, 32, 35–38], while UA-MT, SASSNet, DTC, BCP, and MCF were selected as alternative models representing different approaches, such as uncertainty estimation, geometric shape regularity, task-level regularization, bidirectional CutMix, and model-level regularization. Notably, when applied to pancreas segmentation using the Pancreas-NIH dataset, our PMT model yielded a 7.17% improvement in DSC, a 9.09% improvement in IoU index, a reduction of 6.35 in 95HD, and a reduction of 2.10 in ASD. Motivated by these significant advancements, we ventured to employ the PMT model for maxillary sinus segmentation, successfully achieving comparable and encouraging results.

In this study, the correlation of maxillary sinus's size with age reflected clearly in group under 18 years old that all measured variables had significant linear correlation with age. Comparatively, for 18 and above age group, this correlation was not as pronounced in scatter plots or Pearson's correlation test. Only certain variables—L_MSL, R_MSL, R_MSW, and R_MSH—showed a significant association with age. This suggested that the rate of development of the maxillary sinus in minors is significantly faster than the rate of decline in adulthood.

To estimate age, we utilized these significant variables and applied two different methods: multiple linear regression and random forest. Surprisingly, the multiple linear regression models outperformed the random forest models in both age groups. This suggested that for linear correlations, traditional statistical methods may be more appropriate than machine learning techniques. It was possible that the relatively small sample size or the presence of substantial noise due to numerous influencing factors, including the effect of gender differences, led to overfitting in the machine learning models. To address this, future research should aim to increase the sample

Table 3 Descriptive statistics of maxillary sinus data

Variable		Sex	Mean ± SD(mm/mm3)	Min(mm/mm^3)	Max(mm/mm^3)
Under 18 years old	L_MSL	male	37.54 ± 2.79	32.14	44.94
		female	37.18 ± 2.55	32.11	44.25
	L_MSW	male	31.74 ± 3.05	24.46	38.13
		female	31.68 ± 3.11	24.12	38.25
	L_MSH	male	36.28 ± 5.01	23.80	48.73
		female	36.03 ± 4.54	23.48	48.68
	R_MSL	male	37.58 ± 2.53	30.77	42.21
		female	37.15 ± 2.42	31.45	43.18
	R_MSW	male	32.49 ± 2.87	25.41	37.87
		female	31.83 ± 2.80	25.76	37.41
	R_MSH	male	35.72 ± 4.61	22.02	48.37
		female	36.00 ± 4.25	26.71	45.65
	L_volume	male	12200.06 ± 4178.57	1801.31	24009.83
		female	13402.95 ± 3444.85	4783.43	23104.28
	R_volume	male	14872.11 ± 4048.64	6168.58	26814.86
		female	15136.20 ± 3729.73	6173.28	24970.25
	distance	male	87.92 ± 5.88	73.27	100.43
		female	86.41 ± 6.07	72.91	98.13
Aged 18 and above	L_MSL	male	39.05 ± 4.18	25.13	52.15
		female	36.38 ± 3.12	28.20	43.29
	L_MSW	male	32.45 ± 4.48	19.96	40.41
		female	30.49 ± 3.86	22.12	39.55
	L_MSH	male	39.59 ± 7.34	17.56	52.36
		female	35.87 ± 5.66	23.40	54.83
	R_MSL	male	38.00 ± 3.80	28.41	44.40
		female	35.61 ± 3.29	25.28	42.65
	R_MSW	male	32.71 ± 4.56	21.96	41.78
		female	30.32 ± 3.97	21.09	39.71
	R_MSH	male	39.93 ± 7.41	15.90	51.55
		female	35.83 ± 5.05	23.88	48.09
	L_volume	male	14453.02 ± 6534.85	1699.54	28175.63
		female	11944.19 ± 4516.56	2032.05	21060.76
	R_volume	male	18395.72 ± 6807.19	5004.56	32198.93
		female	14877.50 ± 4563.76	4303.21	30296.27
	distance	male	91.11 ± 7.79	69.65	105.83
		female	85.49 ± 6.91	67.03	104.80

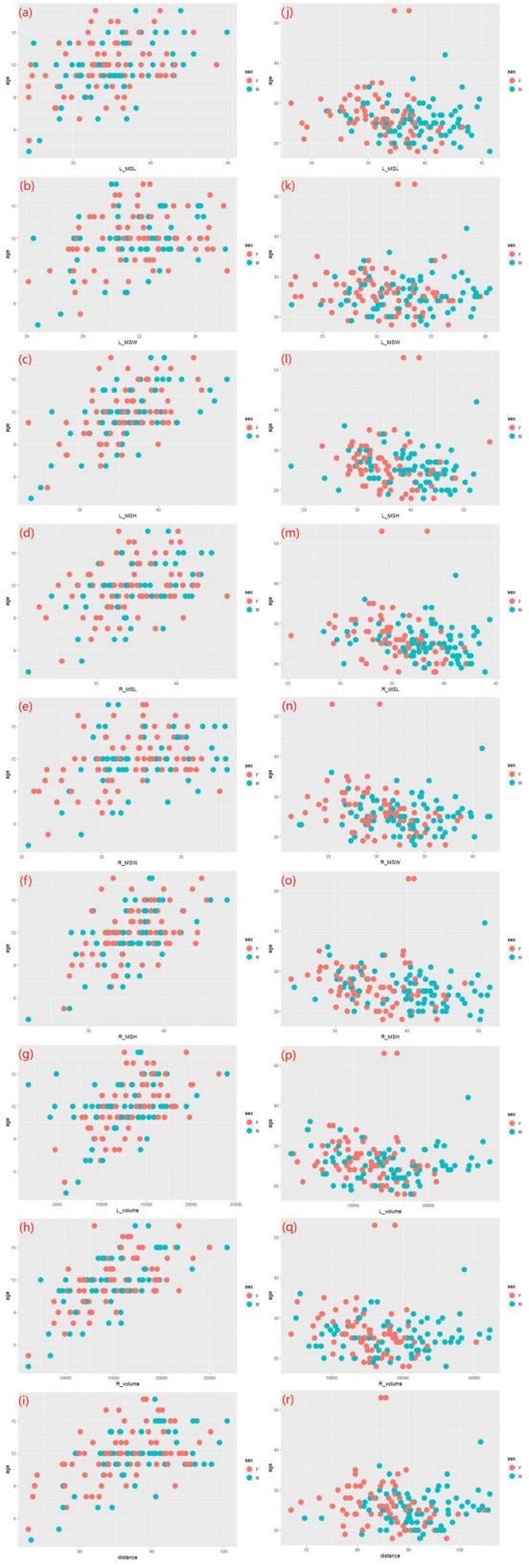

Fig. 5 Scatterplot of each variable

Table 4 Test results of different models in two groups

Group	Model type	Model parameters	MAE
Under 18 years old	multiple linear regression	age = 2.8444815 − 0.0769627*L_MSL-0.1391167*L_MSW-0.021875*L_MSH-0.1390213*R_MSL-0.2690378*R_MSW + 0.1123411*R_MSH-0.0001429*L_volume + 0.0004433*R_volume + 0.2522108*distance	1.45
	random forest	the number of trees = 240; the number of variables tried at each split = 3	1.62
Aged 18 and above	multiple linear regression	age = 36.23741 + 0.25756*L_MSL-0.39550*R_MSL-0.08232*R_MSW-0.07428*R_MSH	3.51
	random forest	the number of trees = 240; the number of variables tried at each split = 1	3.84

Table 5 Comparing with some previous studies

Detection Object	Age range	Model type	MAE
Maxillary Sinus	4–17	multiple linear repression	1.46
	18–53	multiple linear repression	3.61
Clavicle	14–29	machine learning、deep learning	2.08
Sperm-Specific AR-CpG Markers	22–51	svmpoly	2.59
Maxillary Canine、Mandibular First Molar	17–60	multiple linear repression	2.76

size and re-group the data by considering gender as an influencing factor.

The MAE of testing results in two group were 1.45 and 3.51 years. For comparison, we examined the performance of age estimation models based on other technologies. Deng et al. [8] utilized clavicle to estimate age in individuals aged 14–29, achieving an MAE of 2.08 years (listed in Table 5). However, this method was limited to younger age groups. Huang [39] identified age-related markers in sperm and estimated age by measuring their methylation levels, achieving an MAE of 2.59 years in individuals aged 22–51 with the help of machine learning and deep learning (shown in Table 5). The complexity of this method and its reliance on advanced facilities and high-quality samples constrained its widespread application. In Ilayaraja's study [40], the samples ranged from 17 to 60 years old. By analyzing the images of maxillary canine and mandibular first molar, an MAE of just 2.76 years was achieved (refer to Table 5). Teeth, with their stability and age-related changes such as wear and tear and secondary dentin deposition, are excellent for individual identification in forensic science. Advances in image technology enable cost-effective measurement of tooth data, which can be automated using the segmentation model described above. Therefore, an age estimation model that combines measurements from both the maxillary sinus and teeth is hypothesized to offer increased accuracy. This hypothesis will be validated in subsequent research.

Conclusion

In conclusion, the age estimation model utilizing the maxillary sinus has proven to be a valuable tool, particularly in scenarios where the age of adults needs to be determined. And the automatic segmentation model for the maxillary sinus demonstrated its capability to collect data rapidly and accurately. Our research has successfully fitted two robust models using linear data and volume measurements obtained from CBCT scans of the Han population, achieving the MAE of 1.45 years for individuals under 18 years old and 3.51 years for those aged 18 and above. Further studies will focus on integrating additional estimating bases, such as dental measurements with the maxillary sinus to achieve higher accuracy.

Abbreviations

CT	Computed Tomography
CBCT	Cone Beam Computed Tomography
PMT	Progressive Mean Teacher
MSL	length of maxillary sinus
MSW	width of maxillary sinus
MSH	height of maxillary sinus
Distance	distance of lateral wall between two maxillary sinuses
SSL	semi-supervised learning
DSC	Dice Similarity Coefficient
IoU	Intersection over Union
95HD	95% Hausdorff Distance
ASD	Average Surface Distance
MAE	mean absolute error

Acknowledgements

Not Applicable.

Author contributions

Y.X. Guo and J.L. Lan contributed to conception and design of the study, drafted the manuscript; H.Y. Yue contributed to the training of automatic Maxillary Sinus segmentation model; W.Q. Bu, Y.T, D.W, H.Y, J.C. Ren and Y.X. Song participated in data analysis, and experimental technical support; H.T. Meng contributed to conception of the study, and critically revised the manuscript; Y.C. Guo and Y.X. Guo designed this research, critically revised the manuscript, provided fund support. All authors agreed to be accountable for all aspects of the work.

Funding

This work was supported by the Young Science and Technology Star Program of Shaanxi Province of China (2020KJXX-025), the National Natural Science Foundation of China (No. 82402206, 81701869) and National Training Program of Innovation and Entrepreneurship for Undergraduates (S202310698646). We express our gratitude to Ning Gao and Hong-Ying Yue for their generous contribution of the maxillary sinus segmentation technique, which was instrumental in the training phase of our research.

Data availability

The datasets used and analyzed during the current study are available from the corresponding author on reasonable request.

Declarations

Ethics approval and consent to participate
The ethical standards of the institutional and/or national research committee and the 1964 Declaration of Helsinki and its later amendments or comparable ethical standards were followed in the whole process involving volunteers. The current research was conducted after the approval of the Biomedical Ethics Committee of Xi'an Jiaotong University Health Science Center, China (No: [2021] 1473). Meanwhile, volunteers' CBCT were further collected after the acquisition of written informed consents.

Consent for publication
Not applicable.

Competing interests
The authors declare no competing interests.

Received: 3 September 2024 / Accepted: 10 February 2025
Published online: 26 February 2025

References

1. Ubelaker DH, Shamlou A, Kunkle A. Contributions of forensic anthropology to positive scientific identification: a critical review. Forensic Sci Res. 2019;4(1):45–50.
2. Schmeling A, et al. Forensic age estimation. Dtsch Arztebl Int. 2016;113(4):44–50.
3. Boldsen JL, Milner GR, Ousley SD. Paleodemography: from archaeology and skeletal age estimation to life in the past. Am J Biol Anthropol. 2022;178(Suppl 74):115–50.
4. Gumpangseth T, Mahakkanukrauh P. Age estimation in the combined long bones and ribs by histomorphometry: past, present, and future. Med Sci Law. 2024;64(1):52–71.
5. Pinto PHV, Fares LC, Silva R. Dental age estimation by cementum incremental lines counting: a systematic review and meta-analysis. Forensic Sci Int. 2022;341:111492.
6. Smith DEM, Humphrey LT, Cardoso HFV. Age estimation of immature human skeletal remains from mandibular and cranial bone dimensions in the postnatal period. Forensic Sci Int. 2021;327:110943.
7. Le Clercq LS, et al. Biological clocks as age estimation markers in animals: a systematic review and meta-analysis. Biol Rev Camb Philos Soc. 2023;98(6):1972–2011.
8. Qiu L, et al. Machine learning and deep learning enabled age estimation on medial clavicle CT images. Int J Legal Med. 2024;138(2):487–98.
9. Buikstra JE, Ubelaker DH. *Standards for data collection from human skeletal remains: proceedings of a seminar at the field museum of natural history. Documentation of sex differences and age changes in adults.* Arkansas Archeological Survey, 1994.
10. Phenice TW. A newly developed visual method of sexing the os pubis. Am J Phys Anthropol. 1969;30(2):297–301.
11. Burr DB. The anatomy and biology of the human skeleton. J Hum Evol. 1989;18(3):288–9.
12. Spradley MK, Jantz RL. Sex estimation in forensic anthropology: skull versus postcranial elements. J Forensic Sci. 2011;56(2):289–96.
13. Hattori N, Liu YY, Ushijima T. DNA Methylation Anal Methods Mol Biol. 2023;2691:165–83.
14. Singer BD. A practical guide to the measurement and analysis of DNA methylation. Am J Respir Cell Mol Biol. 2019;61(4):417–28.
15. Uthman AT, et al. Evaluation of maxillary sinus dimensions in gender determination using helical CT scanning. J Forensic Sci. 2011;56(2):403–8.
16. Amin MF, Hassan EI. Sex identification in Egyptian population using Multidetector Computed Tomography of the maxillary sinus. J Forensic Leg Med. 2012;19(2):65–9.
17. Ekizoglu O, et al. The use of maxillary sinus dimensions in gender determination: a thin-slice multidetector computed tomography assisted morphometric study. J Craniofac Surg. 2014;25(3):957–60.
18. Teke HY, et al. Determination of gender by measuring the size of the maxillary sinuses in computerized tomography scans. Surg Radiol Anat. 2007;29(1):9–13.
19. Dangore-Khasbage S, Bhowate R. Utility of the morphometry of the maxillary sinuses for gender determination by using computed tomography. Dent Med Probl. 2018;55(4):411–7.
20. Przystańska A, et al. Sexual dimorphism of maxillary sinuses in children and adolescents - a retrospective CT study. Ann Anat. 2020;229:151437.
21. Lorkiewicz-Muszyńska D, et al. Development of the maxillary sinus from birth to age 18. Postnatal growth pattern. Int J Pediatr Otorhinolaryngol. 2015;79(9):1393–400.
22. Otsuki K, et al. Development of New Formulas for Sex and Age Estimation by assessing Maxillary Sinus morphology on CBCT. Yonago Acta Med. 2023;66(1):112–9.
23. Sahu A, Mishra J, Kushwaha N. Artificial Intelligence (AI) in drugs and pharmaceuticals. Comb Chem High Throughput Screen. 2022;25(11):1818–37.
24. Niazi MKK, Parwani AV, Gurcan MN. Digital pathology and artificial intelligence. Lancet Oncol. 2019;20(5):e253–61.
25. Rizve MN, Kardan N, Shah M. Towards realistic semi-supervised learning. Cham: Springer; 2022.
26. Cheplygina V, de Bruijne M, Pluim JPW. Not-so-supervised: a survey of semi-supervised, multi-instance, and transfer learning in medical image analysis. Med Image Anal. 2019;54:280–96.
27. Huynh T, Nibali A, He Z. Semi-supervised learning for medical image classification using imbalanced training data. Comput Methods Programs Biomed. 2022;216:106628.
28. Sun P, et al. MTAN: a semi-supervised learning model for kidney tumor segmentation. J Xray Sci Technol. 2023;31(6):1295–313.
29. Ronneberger O, Fischer P, Brox T. U-Net: Convolutional Networks for Biomedical Image Segmentation. Cham: Springer International Publishing; 2015.
30. Zhang G, et al. Automatic segmentation of organs at risk and tumors in CT images of lung cancer from partially labelled datasets with a semi-supervised conditional nnu-net. Comput Methods Programs Biomed. 2021;211:106419.
31. Bai Y et al. *Bidirectional copy-paste for semi-supervised medical image segmentation*. in *Proceedings of the IEEE/CVF conference on computer vision and pattern recognition*. 2023.
32. Wang Y et al. *Mcf: Mutual correction framework for semi-supervised medical image segmentation*. in *Proceedings of the IEEE/CVF conference on computer vision and pattern recognition*. 2023.
33. Gao N, et al. PMT: Progressive Mean Teacher via exploring temporal consistency for Semi-supervised Medical Image Segmentation. Cham: Springer Nature Switzerland; 2025.
34. Schwendicke F, et al. Artificial intelligence in dental research: Checklist for authors, reviewers, readers. J Dent. 2021;107:103610.
35. Yu L et al. *Uncertainty-aware self-ensembling model for semi-supervised 3D left atrium segmentation*. in *Medical image computing and computer assisted intervention–MICCAI 2019: 22nd international conference, Shenzhen, China, October 13–17*, 2019, proceedings, part II 22. 2019. Springer.
36. Li S, Zhang C, He X. *Shape-aware semi-supervised 3D semantic segmentation for medical images*. in *Medical Image Computing and Computer Assisted Intervention–MICCAI* 2020: 23rd International Conference, Lima, Peru, October 4–8, 2020, Proceedings, Part I 23. 2020. Springer.
37. Luo X et al. *Semi-supervised medical image segmentation through dual-task consistency*. in *Proceedings of the AAAI conference on artificial intelligence*. 2021.
38. Yun S et al. *Cutmix: Regularization strategy to train strong classifiers with localizable features*. in *Proceedings of the IEEE/CVF international conference on computer vision*. 2019.
39. Xiao C, et al. Improved age estimation from semen using sperm-specific age-related CpG markers. Forensic Sci Int Genet. 2023;67:102941.
40. Ilayaraja V, et al. Digitized Morphometric Analysis using Maxillary Canine and Mandibular First Molar for Age Estimation in South Indian Population. Open Dent J. 2018;12:762–9.

Publisher's note